

Quantum chaos and fractals with atoms in cavities

M. Uleysky, L. Kon'kov, S. Prants

*Laboratory of Nonlinear Dynamical Systems, V.I.Il'ichev Pacific Oceanological
Institute of the Russian Academy of Sciences, 690041 Vladivostok, Russia*

Abstract

We study the coupled translational, electronic, and field dynamics of the combined system “a two-level atom + a single-mode quantized field + a standing-wave ideal cavity”. In the semiclassical approximation with a point-like atom, interacting with the classical field, the dynamics is described by the Heisenberg equations for the atomic and field expectation values which are known to produce semiclassical chaos under appropriate conditions. We derive Hamilton – Schrödinger equations for probability amplitudes and averaged position and momentum of a point-like atom interacting with the quantized field in a standing-wave cavity. They constitute, in general, an infinite-dimensional set of equations with an infinite number of integrals of motion which may be reduced to a dynamical system with four degrees of freedom if the quantized field is supposed to be initially prepared in a Fock state. This system is found to produce semiquantum chaos with positive values of the maximal Lyapunov exponent. At exact resonance, the semiquantum dynamics is regular. At large values of detuning $|\delta| \gg 1$, the Rabi atomic oscillations are usually shallow, and the dynamics is found to be almost regular. The Doppler – Rabi resonance, deep Rabi oscillations that may occur at any large value of $|\delta|$ to be equal to $|\alpha p_0|$, is found numerically and described analytically (with α to be the normalized recoil frequency and p_0 the initial atomic momentum). Two gedanken experiments are proposed to detect manifestations of semiquantum chaos in real experiments. It is shown that in the chaotic regime values of the population inversion z_{out} , measured with atoms after transversing a cavity, are so sensitive to small changes in the initial inversion z_{in} that the probability of detecting any value of z_{out} in the admissible interval $[-1, 1]$ becomes almost unity in a short time. Chaotic wandering of a two-level atom in a quantized Fock field is shown to be fractal. Fractal-like structures, typical with chaotic scattering, are numerically found in the dependence of the time of exit of atoms from the cavity on their initial momenta.

Key words: quantum chaos, atomic fractals, cavity QED

PACS: 42.50.Vk, 05.45.Df, 05.45.Mt

1 Introduction

The correspondence between quantum and classical worlds has been a subject of much interest from the early days of quantum mechanics. The emergence of classical dynamical chaos from quantum mechanics is one of the most debated problems in this field [1]. *Isolated and bounded* quantum systems do not show sensitive dependence on initial conditions in the same way as classical systems due to discreteness of quantum phase space and lacking of notion of trajectories in quantum mechanics. The Schrödinger equation for an isolated quantum system demonstrates only (quasi)periodic solutions even if the classical counterpart of the quantum system under consideration would be chaotic. However, it is valid only if the quantum system is assumed to be absolutely isolated from the surroundings.

In this paper, we study the temporal evolution of the strongly coupled atom-field system consisting of a single two-level atom interacting with a single mode of the quantized field in a standing-wave ideal cavity without any leakage of photons. If the atom is assumed to be at rest the respective Jaynes – Cummings Hamiltonian is known to be integrable in the rotating-wave approximation both under fully quantum and semiclassical descriptions [2]. If the atom moves with a constant velocity (the Raman – Nath approximation) in the direction along which the coefficient of the atom-field coupling is changed (say, periodically) the semiclassical evolution of the expectation values of the atomic and field operators has been shown to be chaotic [3,4,5] with positive values of the maximal Lyapunov exponent in respective ranges of control parameters. The same time-periodic Hamiltonian has been shown to generate quasiperiodic solutions of the respective time-dependent Schrödinger equation for the probability amplitudes [6]. The Jaynes – Cummings system possesses two degrees of freedom, the electronic (internal) atomic one and the field one. In fact, when emitting and absorbing photons, an atom not only changes its internal state but its velocity is changed as well due to the photon recoil. It is a pronouncing effect with cold atoms in a laser field (see for a review, for example, [7]). Taking into account the translational (external) atomic degree of freedom, we get the autonomous Hamiltonian (1) with three degrees of freedom. The respective semiclassical equations of motion for the expectation values of the atomic position and momentum operators, the atomic population operator, and the combined atom-field operators have been shown to be chaotic [8,9] with positive values of the maximal Lyapunov exponent. The semiclassical atom-field dynamics has been shown to demonstrate many interesting features, including the interaction of nonlinear resonances [10], atomic fractals [5,11], Lévy flights and anomalous atomic diffusion [12], and the Doppler – Rabi resonance [13].

Email address: prants@poi.dvo.ru (M. Uleysky, L. Kon'kov, S. Prants).

In this paper, we go further in quantizing the atom-photon interaction in a standing-wave cavity. The field and internal atomic degrees of freedoms are treated as fully quantum ones obeying the Schrödinger equation. They are coupled to the external atomic degree of freedom obeying the Hamilton equations. Such a quantum-classical hybrid may be considered as a reality-based model of interaction between a quantum system and the surroundings. From the standpoint of dynamical system theory, the hybrid is described by an infinite-dimensional set of nonlinear ODE's with an infinite number of integrals of motion with clear physical meanings (see Eqs. (18) – (21)). Any state of the quantized field may be represented as a superposition of a number of the so-called Fock states $|n\rangle$, where n is the number of photons in the respective state. Any state of a two-level atom is a superposition of its ground and excited states. The Hilbert space of the quantized atom-field subsystem (which should be treated as a whole unity) is an infinite direct sum of two-dimensional subspaces in each of which the so-called number of excitations should be conserved in the process of evolution. The atom-field quantized subsystem evolves in such a way that transitions, belonging to the subspaces with different values of the number of excitations, are forbidden. The main aim of the paper is to investigate the effects of quantization on those properties of the system that produce dynamical chaos.

This paper is organized as follows. In Sec. 2 we introduce the system under consideration and the respective Hamiltonian. In Sec. 3 we derive the Heisenberg equations for the expectation values of the atomic and field operators and review briefly the properties of semiclassical chaos. Our main results are given in Sec. 4 where we derive the Hamilton – Schrödinger equations of motion for a two-level atom in a quantized field, study the quantum Doppler – Rabi resonance, the properties of semiquantum chaos, and atomic fractals in the Fock quantized field.

2 Two-level atom with recoil in a standing-wave cavity

We consider a single two-level atom with the frequency ω_a of an electric dipole transition and mass m_a moving in an ideal cavity which sustains a single standing-wave mode along the axis x with the frequency ω_f and the wave vector k_f . In the strong coupling limit, where the coefficient of the coupling Ω_0 is much greater than all the relaxation rates, the atom-field dynamics may be treated as Hamiltonian with the respective operator

$$\hat{H} = \frac{\hat{P}^2}{2m_a} + \frac{\hbar\omega_a}{2} \hat{\sigma}_z + \hbar\omega_f \hat{a}^\dagger \hat{a} - \hbar\Omega_0 \left(\hat{a}^\dagger \hat{\sigma}_- + \hat{a} \hat{\sigma}_+ \right) \cos k_f \hat{X}, \quad (1)$$

whose summands describe the kinetic and internal energies of the atom, the field energy, and the energy of the atom-field interaction, respectively. The momentum \hat{P} , position \hat{X} , atomic $\hat{\sigma}$, and field \hat{a}, \hat{a}^\dagger operators satisfy the standard commutations relations:

$$[\hat{X}, \hat{P}] = i\hbar, \quad [\hat{\sigma}_\pm, \hat{\sigma}_z] = \mp 2\hat{\sigma}_\pm, \quad [\hat{\sigma}_+, \hat{\sigma}_-] = \hat{\sigma}_z, \quad [\hat{a}, \hat{a}^\dagger] = 1. \quad (2)$$

Operators belonging to different degrees of freedom commute with each other at the same time moment.

In the process of emitting and absorbing photons an atom not only changes its internal electronic state but its external translational state is changed as well due to the photon recoil effect. An interplay between the electronic, translational, and field degrees of freedom of the strongly coupled atom-field system may be described as in the Heisenberg as in the Schrödinger pictures.

3 Heisenberg equations for the atomic and field expectation values and semiclassical dynamics

It is convenient to write down the Heisenberg equations for the following operators:

$$\hat{x} = k_f \hat{X}, \quad \hat{p} = \frac{\hat{P}}{\hbar k_f}, \quad \hat{u} = \frac{\hat{a}^\dagger \hat{\sigma}_- + \hat{a} \hat{\sigma}_+}{\sqrt{\hat{N}}}, \quad \hat{v} = i \frac{\hat{a}^\dagger \hat{\sigma}_- - \hat{a} \hat{\sigma}_+}{\sqrt{\hat{N}}}, \quad \hat{\sigma}_z, \quad (3)$$

where $\hat{N} = \hat{a}^\dagger \hat{a} + (\hat{\sigma}_z + \hat{I})/2$ is a constant operator of the total number of excitations and \hat{I} the identity operator. The derivative of an arbitrary operator \hat{A} with respect to the normalized time $\tau = \Omega_0 t$

$$i\hbar \dot{\hat{A}} = [\hat{A}, \hat{H}] \quad (4)$$

results in the following Heisenberg equations for the operators (3):

$$\begin{aligned} \dot{\hat{x}} &= \alpha \hat{p}, \\ \dot{\hat{p}} &= -\sqrt{\hat{N}} \hat{u} \sin \hat{x}, \\ \dot{\hat{u}} &= \delta \hat{v}, \\ \dot{\hat{v}} &= -\delta \hat{u} + 2\sqrt{\hat{N}} \hat{\sigma}_z \cos \hat{x}, \\ \dot{\hat{\sigma}}_z &= -2\sqrt{\hat{N}} \hat{v} \cos \hat{x}, \end{aligned} \quad (5)$$

where the control parameters

$$\alpha = \frac{\hbar k_f^2}{m_a \Omega_0}, \quad \delta = \frac{\omega_f - \omega_a}{\Omega_0} \quad (6)$$

are the normalized recoil frequency and the detuning between the field and the atomic frequencies, respectively. The parameter $\alpha = 2\omega_R/\Omega_0$ characterizes the average change in translational energy $\hbar\omega_R$ in the process of emission and absorption of a photon. The set (5) is not closed. In order to describe fully quantized dynamics one should write down the equations of motion for all the products of the operators (3) and their functions which, in turn, would generate another operator products and respective equations of motion and so on. This process, in general, generates an infinite hierarchy of operator equations. The simplest way to resolve this problem is to take quantum expectation values over an initial quantum state and to factorize all the operator products in Eqs. (5). In this way one gets the closed dynamical system

$$\begin{aligned} \dot{x} &= \alpha p, \\ \dot{p} &= -\sqrt{N} u \sin x, \\ \dot{u} &= \delta v, \\ \dot{v} &= -\delta u + 2\sqrt{N} z \cos x, \\ \dot{z} &= -2\sqrt{N} v \cos x, \end{aligned} \quad (7)$$

for the classical variables, namely, the atomic position $x = \langle \hat{x} \rangle$ and momentum $p = \langle \hat{p} \rangle$, the atom-field variables $u = \langle \hat{u} \rangle$ and $v = \langle \hat{v} \rangle$, and the atomic population inversion $z = \langle \hat{\sigma}_z \rangle$. A conserved number of excitations in the system $N = \langle \hat{N} \rangle = n + (z + 1)/2$ is the additional control parameter. The set (7) has two integrals of motion

$$W = \frac{\alpha}{2} p^2 - u\sqrt{N} \cos x - \frac{\delta}{2} z, \quad R^2 = u^2 + v^2 + z^2, \quad (8)$$

where W is the conserved total energy and R^2 reflects the conservation of the length of the Bloch vector in the limit of the large number of photons, $n = \langle \hat{a}^\dagger \hat{a} \rangle \gg 1$. The set (7) (with slightly another normalization) has been derived in [8,9].

In deriving Eqs. (7) from an infinite hierarchy of Heisenberg operator equations, we treat an atom as a point particle that may be justified if its momentum is much greater than the photon momentum $\hbar k_f$, i. e. if $|p| \gg 1$. Factorization of all the operator products in the respective operator equations means that we do not take into account either quantum nature of the field or quantum correlations between all the atomic and field degrees of freedom. It is justified if $n \gg 1$. Moreover, the procedure of reducing operator equations to semiclassical ones is not unique because the form of the resulting

semiclassical equations depends on the factorization procedure. Semiclassical equations of motion, different from (7), have been derived in [5,12] with the same Hamiltonian (1). All of them, of course, has the same form in the limit $n \gg 1$.

It has been found in a series of papers [8,9,5,10,12] that the semiclassical equations of motion of the strongly coupled atom-field system in a standing wave cavity produce different types of motion. At exact resonance, $\delta = 0$, the motion is regular since the set (7) gains an additional conserved quantity $u(\tau) = u(0) = u_0$ which reflects the conservation of the atom-field interaction energy at $\delta = 0$. Depending on the values of the initial atomic momentum p_0 , an atom either oscillates periodically in a potential well of the standing wave or flies over its potential hills. In resonance, the optical potential $U = -u_0\sqrt{N}\cos x - \delta z/2$ coincides with the standing wave structure. The oscillations of the internal atomic energy, the so-called Rabi oscillations $z(\tau)$, and the oscillations of the atom-field variables, $u(\tau)$ and $v(\tau)$, are regular as well. The center-of-mass motion of the atom does not depend on the Rabi oscillations, but its frequency depends on the initial interaction energy u_0 since it determines the depth of the optical potential wells. In contrary, the Rabi oscillations depend on the translational motion since the strength of the atom-field coupling depends on the position of an atom in a cavity. The respective exact solutions of Eqs. (7) with $\delta = 0$ one can found in [9].

Out of resonance, $\delta \neq 0$, the set (7) with two integrals (8) is an autonomous Hamiltonian system whose motion takes place on a three-dimensional hypersurface. It has, generally speaking, a positive Lyapunov exponent λ which has been computed in the paper [8] as a function of the control parameters α and δ and of the initial atomic momentum p_0 . It follows from the first two equations in (7) that the atomic center-of-mass motion is described by the equation for a physical pendulum with a frequency modulation

$$\ddot{x} + \alpha\sqrt{N}u(\tau)\sin x = 0, \quad (9)$$

where u is a function of time and all the other variables. Following to [14,10] one can show that Eq. (9) may produce a stochastic layer in a neighbourhood of the unperturbed separatrix. Analogously to what has been done in [10], the normalized (to a separatrix value) width of the stochastic layer may be estimated as follows

$$\Delta \simeq 8\pi (\Omega/\omega)^3 \exp\left(-\frac{\pi\Omega}{2\omega}\right), \quad (10)$$

where $\Omega = \sqrt{\delta^2 + 4N}$ is the normalized Rabi frequency and the frequency $\omega = \sqrt{2\alpha N^{3/2}|\delta|}/\Omega$ characterizes small-amplitude oscillations. It should be noted that Δ gives the lower bound for the layer width (see [10]).

Center-of-mass motion of a two-level atom in an ideal standing-wave cavity has been found in [12] to be anomalous. A typical chaotic atomic trajectory consists of intervals of regular motion with an almost constant velocity in each interval (Lévy flights) interrupted by erratic walks. Such an intermittency is typical of Hamiltonian systems with nonhomogeneous phase space with a fractal-like structure consisting of KAM tori, cantori, chains of islands, stochastic sea, etc. [15]. From this point of view, the Lévy flights may be understood as those trajectories that “stick” to islands boundaries for a long time. The representative point on a typical chaotic trajectory sooner or later approaches, as closely as desirable, an island boundary that separates regular and chaotic motions. Nearby such a boundary, the maximal Lyapunov exponent λ goes to zero, and cantories block the trajectory escape to the stochastic sea. As a result, the atomic motion is almost regular for a time that may be very long. From the physical point of view, the intermittency of the center-of-mass motion is due to the intermittent oscillations of the effective optical potential $U_{\text{eff}} = -\sqrt{N}u \cos x - \delta z/2$ which governs the translational motion of the atom [13].

The Lévy flights impact the statistical properties of the atomic motion resulting in the anomalous diffusion. It was numerically found in [12] that the second moment of the position of atom in a cavity evolves in time as $\bar{x}^2 \sim \tau^\mu$, where the transport exponent μ may vary from the value $\mu \simeq 1$, corresponding to the normal diffusion, to the value $\mu \simeq 2$ corresponding to the superdiffusion. The Poincaré theorem states that every trajectory of a closed conservative dynamical system, except for trajectories of the set of zero measure, returns arbitrarily close to its origin infinitely many times. The recurrence time distribution in the system with perfect mixing is known to be Poissonian, $P(\tau) = h^{-1}e^{-h\tau}$, where h is the Kolmogorov-Sinai entropy. The motion with intermittency and Lévy flights leads to the power law, $P(\tau) \sim \tau^{-\gamma}$ at $\tau \rightarrow \infty$. The exponents μ and γ are related to each other, and their values depends on the values of the control parameters α , δ , and N because by changing them one changes the topology of the phase space.

The atom-photon interaction in a cavity may be considered as the chaotic scattering problem [5,11] where a two-level atom is scattered by the standing-wave light or by an optical potential. In difference from the usual scattering of atoms by light [7], the effective optical potential U_{eff} of the strongly coupled atom-field system depends not only on the field but on the atomic variables as well. Let two atomic detectors to be placed at the cavity mirrors and let them detect the time T of atomic exit from the cavity. Let the identically prepared atoms with given initial momenta p_0 be placed one by one in the middle of the cavity. The dependence $T(p_0)$ has been found in [5,11] to have a beautiful selfsimilar structure with the Hausdorff dimension to be equal to $d \simeq 1.84$. Tiny interplay between all the degrees of freedom is responsible for trapping atoms with $T \rightarrow \infty$ even in a very short microcavity. Simulation in

the cited papers has been performed with a cavity whose length is equal to two standing-wave lengths. Two kinds of atomic fractals have been found in [11], a countable fractal (a set of p_0 generating separatrix-like atomic trajectories) and a seemingly uncountable fractal with a set of p_0 generating infinite walkings of atoms inside the cavity.

4 Hamilton-Schrödinger equations and semiquantum dynamics

4.1 Derivation of equations of motion

In this section we again consider a two-level atom as a point particle but electronic and field degrees of freedom are treated as fully quantum ones in the Schrödinger picture. It enables us to study the role that field quantum statistic and atomic superposition play in the full atom-field dynamics including chaos. We start with the Hamiltonian \hat{H} (1).

The Hamilton equations for the classical translational degree of freedom is easily found

$$\frac{d\langle\hat{X}\rangle}{dt} = \frac{\partial\langle\hat{H}\rangle}{\partial\langle\hat{P}\rangle}, \quad \frac{d\langle\hat{P}\rangle}{dt} = -\frac{\partial\langle\hat{H}\rangle}{\partial\langle\hat{X}\rangle}, \quad (11)$$

where $\langle\dots\rangle$ denotes an expectation value of the corresponding operator over a quantum state $|\Psi\rangle$ of the electronic-field Hamiltonian. Using the same normalizations and notations as in the preceding section, we get

$$\dot{x} = \alpha p, \quad \dot{p} = -\langle\hat{u}\rangle \sin x, \quad (12)$$

where $\langle\hat{u}\rangle = \langle\Psi(\tau)|\hat{u}_0|\Psi(\tau)\rangle$.

Let us expand a state vector of the electronic-field subsystem over the basic energetic atomic states $|2\rangle$ and $|1\rangle$ and the Fock field states $|n\rangle$

$$|\Psi(\tau)\rangle = \sum_{n=0}^{\infty} \left(a_n(\tau)|2, n\rangle + b_n(\tau)|1, n\rangle \right), \quad (13)$$

where a_n and b_n are the probability amplitudes to find the atom in its excited or ground state with n photons in the mode, respectively. Substitution of the vector (13) in the time-dependent Schrödinger equation

$$i\hbar|\dot{\Psi}\rangle = \hat{H}|\Psi\rangle \quad (14)$$

gives the infinite-dimensional set of the coupled ODE's

$$\begin{aligned}\dot{a}_n &= -i \left(\Delta_a a_n - \sqrt{n+1} b_{n+1} \cos x \right), \\ \dot{b}_{n+1} &= i \left(\Delta_b b_{n+1}^* - \sqrt{n+1} a_n^* \cos x \right), \quad n = 0, 1, 2, \dots,\end{aligned}\quad (15)$$

where $\Delta_a = n\omega_f + \omega_a/2$ and $\Delta_b = (n+1)\omega_f - \omega_a/2$. Introducing the following combinations of the probability amplitudes:

$$u_n = 2 \operatorname{Re} \left(a_n b_{n+1}^* \right), \quad v_n = -2 \operatorname{Im} \left(a_n b_{n+1}^* \right), \quad z_n = |a_n|^2 - |b_{n+1}|^2, \quad (16)$$

we get the quantum Bloch-like equations

$$\begin{aligned}\dot{u}_n &= \delta v_n, \\ \dot{v}_n &= -\delta u_n + 2\sqrt{n+1} z_n \cos x, \\ \dot{z}_n &= -2\sqrt{n+1} v_n \cos x, \quad n = 0, 1, 2, \dots,\end{aligned}\quad (17)$$

where the detuning δ is the same as in (6). After computing $\langle \hat{u} \rangle$, we obtain our basic Hamilton-Schrödinger equations

$$\begin{aligned}\dot{x} &= \alpha p, \\ \dot{p} &= -\sum_{n=0}^{\infty} \sqrt{n+1} u_n \sin x, \\ \dot{u}_n &= \delta v_n, \\ \dot{v}_n &= -\delta u_n + 2\sqrt{n+1} z_n \cos x, \\ \dot{z}_n &= -2\sqrt{n+1} v_n \cos x, \quad n = 0, 1, 2, \dots\end{aligned}\quad (18)$$

This infinite set of *nonlinear* ODE's possesses an infinite number of the integrals of motion, the total energy integral

$$W = \frac{\alpha}{2} p^2 - \sum_{n=0}^{\infty} \sqrt{n+1} u_n \cos x - \frac{\delta}{2} \sum_{n=0}^{\infty} z_n, \quad (19)$$

the Bloch-like integrals for each n

$$R_n^2 = u_n^2 + v_n^2 + z_n^2, \quad (20)$$

and the global integral reflecting conservation of the total probability

$$\sum_{n=0}^{\infty} R_n = 1. \quad (21)$$

The quantities that can be measured in real experiments are the atomic position x , momentum p and the atomic population inversion

$$z(\tau) = \sum_{n=0}^{\infty} z_n(\tau). \quad (22)$$

The semiquantum equations (18) – (21) should be compared with the semiclassical equations (7) and (8) because they describe the same physical situation but on the different ground. They are exactly identical in the case of the initial Fock state of the cavity field with \bar{n} quanta and the atom to be prepared initially in one of its energetic states. It is easy to show that an infinite number of equations (18) reduces in this case to five equations (7) with $N = \bar{n} + (z + 1)/2 = \bar{n} + 1$ if $|\Psi(0)\rangle = |2, n\rangle$ and $N = \bar{n}$ if $|\Psi(0)\rangle = |1, n\rangle$. If the atom is initially prepared in a general superposition state and the field is in the Fock state $|n\rangle$

$$|\Psi(0)\rangle = a_n(0)|2, n\rangle + b_n(0)|1, n\rangle, \quad |a_n(0)|^2 + |b_n(0)|^2 = 1, \quad (23)$$

we get from Eqs. (18)

$$\begin{aligned} \dot{x} &= \alpha p, \\ \dot{p} &= -\left(\sqrt{\bar{n}} u_{n-1} + \sqrt{\bar{n} + 1} u_n\right) \sin x, \\ \dot{u}_{n-1} &= \delta v_{n-1}, & \dot{u}_n &= \delta v_n, \\ \dot{v}_{n-1} &= -\delta u_{n-1} + 2\sqrt{\bar{n}} z_{n-1} \cos x, & \dot{v}_n &= -\delta u_n + 2\sqrt{\bar{n} + 1} z_n \cos x, \\ \dot{z}_{n-1} &= -2\sqrt{\bar{n}} v_{n-1} \cos x, & \dot{z}_n &= -2\sqrt{\bar{n} + 1} v_n \cos x \end{aligned} \quad (24)$$

with the respective integrals

$$\begin{aligned} W &= \frac{\alpha}{2} p^2 - \left(\sqrt{\bar{n}} u_{n-1} + \sqrt{\bar{n} + 1} u_n\right) \cos x - \frac{\delta}{2} (z_{n-1} + z_n), \\ R_{n-1}^2 &= u_{n-1}^2 + v_{n-1}^2 + z_{n-1}^2 = |b_n(0)|^4, \\ R_n^2 &= u_n^2 + v_n^2 + z_n^2 = |a_n(0)|^4, \\ R_{n-1} + R_n &= 1, \end{aligned} \quad (25)$$

and initial conditions

$$\begin{aligned} x(0) &= x_0, \quad p(0) = p_0, \quad z_{n-1}(0) = -|b_n(0)|^2, \quad z_n(0) = |a_n(0)|^2, \\ u_{n-1}(0) &= u_n(0) = v_{n-1}(0) = v_n(0) = 0. \end{aligned} \quad (26)$$

4.2 Doppler – Rabi resonance

If the field frequency ω_f is far detuned from the frequency of the atomic working transition ω_a , i. e. if $|\delta| \gg 1$, then the Rabi oscillations $z(\tau)$ should be very shallow as oscillations of an oscillator under influence of a far-detuned time-dependent force. It is correct if the atom does not move. The Doppler effect with a moving atom causes an interesting effect of the Doppler – Rabi resonance if the condition $|\alpha p| \simeq |\delta|$ is fulfilled. A standing wave is a sum of

two running waves moving in the opposite directions. In the reference frame of the moving atom, their frequencies are different due to the Doppler effect

$$\omega_1 = \omega_f - \frac{v_a}{c} \omega_f, \quad \omega_2 = \omega_f + \frac{v_a}{c} \omega_f, \quad (27)$$

where v_a and c are the atomic and light velocities, respectively, and $v_a \ll c$. If the initial atomic momentum p_0 is sufficiently large, the Raman – Nath condition, $p \simeq p_0$ is valid. Let us define dimensionless detunings between the frequencies of the atomic transition and the running waves as follows:

$$\delta_1 = \frac{\omega_1 - \omega_a}{\Omega_0} = \delta - \alpha p_0, \quad \delta_2 = \frac{\omega_2 - \omega_a}{\Omega_0} = \delta + \alpha p_0. \quad (28)$$

It is evident that the atom comes in resonance with one of the running waves if $|\alpha p_0| \simeq |\delta|$. If $|\delta| \gg 1$, the interaction of the atom with the other running wave is negligibly small. Suppose that the atom is initially prepared in the ground state, i. e. $z_{n-1}(0) = -1$, $z_n(0) = 0$, and $z(0) = -1$, than the equations of motion (24) for the atom with a constant speed and with the other initial conditions written in (26) are reduced to the following simple set:

$$\begin{aligned} \dot{u}_n &= \delta v_n, \\ \dot{v}_n &= -\delta u_n + \sqrt{\bar{n} + 1} z_n, \\ \dot{z}_n &= -\sqrt{\bar{n} + 1} v_n. \end{aligned} \quad (29)$$

It should be noted that the amplitude of the running wave is half of the standing-wave amplitude, and the atom-field interaction does not depend on atomic position. The solution for the atomic population inversion with given initial conditions is easy to find

$$z(\tau) = z_n(\tau) = - \left(\frac{\delta - \alpha p_0}{\Omega_n} \right)^2 - \frac{\sqrt{\bar{n} + 1}}{\Omega_n^2} \cos \Omega_n \tau, \quad (30)$$

where $\Omega_n = \sqrt{(\delta - \alpha p_0)^2 + \bar{n} + 1}$ is the Rabi frequency. In particular, at exact Doppler – Rabi resonance, $|\alpha p_0| = |\delta|$, the inversion oscillates at the frequency $(\bar{n} + 1)^{1/4}$ and its amplitude is maximal.

The Doppler – Rabi resonance is illustrated in Fig. 1 where we plot the Rabi oscillation signals $z(\tau)$ computed with the full set (24) and two initial states of the atom when it is prepared in the ground level with $z(0) = -1$ and in the superposition state with $z(0) = 0$ ($z_{n-1}(0) = -1/2$, and $z_n(0) = 1/2$). In our simulation $\alpha = 10^{-3}$, $\bar{n} = 10$ and $x_0 = 0$. When $\delta = 32$ and $p_0 = 32000$ and the resonance condition is fulfilled we really see the maximal Rabi oscillations with both the initial conditions. The signal in Fig. 1a with $z(0) = -1$ is described by the analytical solution (30). When $z(0) = 0$ we have two oscillators with different frequencies (see (24)) and the resulting signal $z(\tau) = z_{n-1}(\tau) + z_n(\tau)$ in Fig. 1c demonstrates a beating with two harmonic components of the type

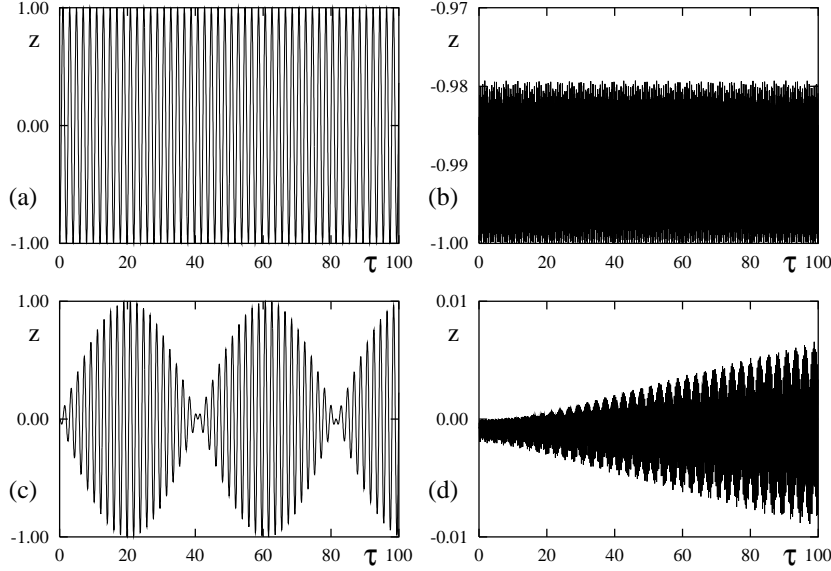


Fig. 1. Doppler – Rabi resonance at the condition $\alpha p_0 = \delta$ with $\delta = 32$, $p_0 = 32000$, $\alpha = 0.001$, (a) $z(0) = -1$ and (c) $z(0) = 0$. Shallow Rabi oscillations with the same value of p_0 but out off the resonance are shown for comparison with (b) $z(0) = -1$, $\delta = 1$ and (d) $z(0) = 0$, $\delta = 10$.

of (30) with $\Omega_n = (\bar{n} + 1)^{1/4}$ and $\Omega_{n-1} = \bar{n}^{1/4}$. For comparison, we plot in Fig. 1b and d very shallow Rabi oscillations with the same value of the atomic momentum $p_0 = 32000$ but out off the resonance, $|\alpha p_0| \neq |\delta|$. The amplitude of the Rabi oscillations in Fig. 1b with $z(0) = -1$ and $\delta = 1$ does not exceed 2% of the amplitude of the resonant oscillations in Fig. 1a. The same is valid with another initial value of the atomic inversion population, $z(0) = 0$ (compare, please, Figs. 1c and d).

In conclusion, deep Rabi oscillations are possible at as large values of the detuning $|\delta|$ as desirable if a two-level atom moves with the corresponding velocity.

4.3 Chaos in a quantized Fock field

Lyapunov exponents are known to be quantitative indicators of chaos in dynamical systems. They characterize the behavior of close trajectories in phase space. If the quantized field is initially prepared in a Fock state $|n\rangle$ with n quanta in the mode, the Hamilton – Schrödinger equations of motion have the form (24) for an arbitrary internal atomic state. The 8-dimensional dynamical system (24) with 4 integrals of motion (25) has, as maximum, four nonzero

Lyapunov exponents λ_i ($i = 1, 2, 3, 4$)

$$\lambda_i = \lim_{\tau \rightarrow \infty} \lambda_i(\tau), \quad \lambda_i(\tau) = \lim_{\Delta_i(0) \rightarrow 0} \frac{1}{\tau} \ln \frac{\Delta_i(\tau)}{\Delta_i(0)}, \quad (31)$$

where $\Delta_i(\tau)$ is the distance (in the Euclidean sense) in the i -th direction at the moment τ between two trajectories that were close to each other at $\tau = 0$. In Hamiltonian systems, due to the phase space volume conservation, $\lambda_1 + \lambda_2 + \lambda_3 + \lambda_4 = 0$, and $\lambda_1 = -\lambda_2$, $\lambda_3 = -\lambda_4$. Computing the maximal Lyapunov exponent λ , one measures an averaged rate of separation of initially close trajectories.

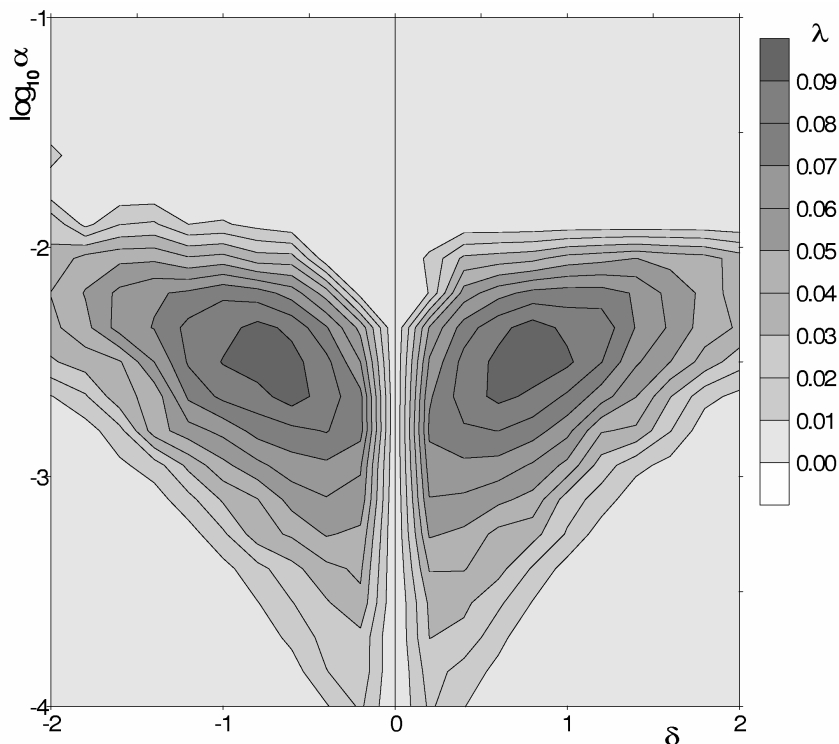


Fig. 2. The maximal Lyapunov exponent λ with zero initial atomic population inversion $z(0) = 0$ and $\bar{n} = 10$ photons in the Fock quantized field versus the atom-field detuning δ and the logarithm of the dimensionless recoil frequency α .

The system has three control parameters, the initial number of photons in the mode \bar{n} , the normalized recoil frequency α and the detuning δ , each of which may vary in a wide range of values. To diagnose chaos it is instructive to compute the so-called topographic λ -maps [3,4,17] which show by color modulation values of λ in the ranges of values of two control parameters with the other to be fixed. When computing the λ -maps, we choose the following initial conditions: $x(0) = 0$, $p(0) = 50$, $u_{n-1}(0) = u_n(0) = v_{n-1}(0) = v_n(0) = 0$, $z_{n-1}(0) = -1/2$, $z_n(0) = 1/2$ and $z_{n-1}(0) = 0$, $z_n(0) = 1$. It means that the atom is prepared initially in the state with zero population inversion $z(0) = 0$ or in the excited state, $z(0) = 1$. In Fig. 2 we show the λ -map with $z(0) = 0$ in

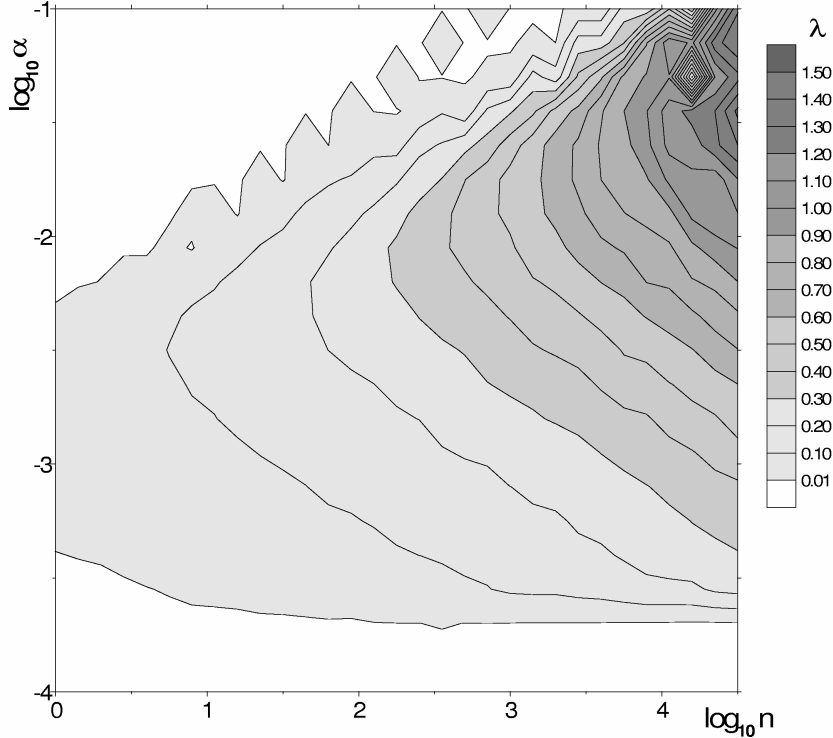


Fig. 3. The double logarithmic plot of λ with an initially excited atom $z(0) = 1$ and $\bar{n} = 10$ photons in the Fock quantized field versus α and \bar{n} with $\delta = 0.5$.

the ranges of the detuning $|\delta| \leq 2$ and the recoil frequency $-4 \leq \log_{10} \alpha \leq -1$ with the fixed value of the initial number of photons $\bar{n} = 10$. The set (24) is integrable at exact atom-field resonance ($\delta = 0$) with $\lambda = 0$. The α - δ map confirms this conjecture. The values of $\alpha \sim 10^{-4} \div 10^{-2}$, that correspond to positive values of λ , are reasonable with real atoms [9], and one may expect chaotic atomic motion in the respective ranges of α and δ . Another λ -map with $z(0) = 1$ shows in Fig. 3 the value of λ in dependence on α and \bar{n} at $\delta = 0.5$ in double logarithmic scale. The magnitude of λ grows, in average, with increasing the initial number of photons in the cavity mode.

A feasible scheme for detecting manifestation of chaos with hot two-level Rydberg atoms moving in a high-Q microwave cavity has been proposed in [5]. The same idea could be realized with cold usual atoms in a high-Q microcavity. Consider a 2D-geometry of a gedanken experiment shown in Fig. 4a, where a monokinetic atomic beam propagates almost perpendicularly to the cavity axis x . In a reference frame moving with a constant velocity in the y -direction, there remains only the transverse atomic motion along the axis x . One measures atomic population inversion after passing the interaction zone. Before injecting atoms in the cavity, it is necessary to prepare all the atoms in the same electronic state, say, in the excited state, with the help of a π -pulse of the laser radiation. It may be done with *only a finite accuracy*, say, equal to Δz_{in} for the initial population inversion z_{in} . The values of the pop-

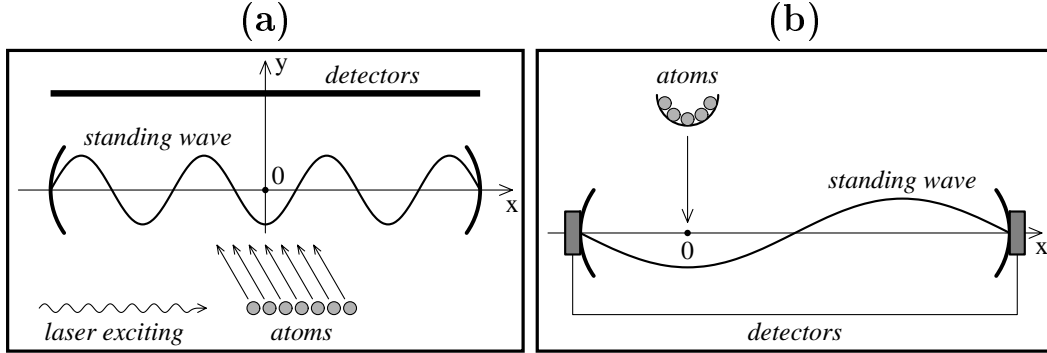


Fig. 4. Schematic diagrams showing scattering of atoms at the standing wave. (a) A monokinetic beam of atoms propagates transversally to the cavity axis x , and the atoms are detected outside the cavity. (b) Atoms are placed one by one inside the cavity with almost zero transversal velocity and are detected at the cavity mirrors.

ulation inversion z_{out} are measured with detectors at a fixed time moment. If we would work with the values of the control parameters corresponding to the regular atom-field dynamics, we would expect to have a regular curve $z_{\text{out}}-z_{\text{in}}$. In the chaotic regime, the atomic inversion at the output can be predicted (within a certain confidence interval Δz) for a time not exceeding the so-called predictability horizon

$$\tau_p \simeq \frac{1}{\lambda} \ln \frac{\Delta z}{\Delta z_{\text{in}}}, \quad (32)$$

which depends weakly on Δz_{in} and Δz . Since the maximal confidence interval lies in the range $|\Delta z| \leq 1$ and λ may reach the values of the order of 1.5 (see λ -maps), the predictability horizon in accordance with the formula (32) can be very short: with $\lambda = 0.5$ τ_p may be of the order of 10 in units of the reciprocal of the vacuum Rabi frequency Ω_0 that correspond to $t_p \simeq 10^{-7}$ s with the realistic value of $\Omega_0 \simeq 10^8$ rad·s $^{-1}$ [18].

In the regular regime, the inevitable errors in preparing Δz_{in} produce the output errors Δz_{out} of the same order. In the chaotic regime, the initial uncertainty increases exponentially resulting in a complete uncertainty of the detected population inversion in a reasonable time. It is demonstrated in Fig. 5, where we plot the dependence of the values of $z(\tau) = z_{\text{out}}$ at $\tau = 100$ (Fig. 5a) and $\tau = 200$ (Fig. 5b) on the values of $z(0) = z_{\text{in}}$ in the chaotic regime with $\delta = 0.4$ and $\lambda \simeq 0.05$. It is evident from Fig. 5a, that at the detection time moment $\tau = 100$ an initial error $\Delta z_{\text{in}} = 10^{-4}$ leads to a complete uncertainty $\Delta z_{\text{out}} \simeq 2$ in rather large vicinities of the initial inversion $z_{\text{in}} \simeq \pm 1$, whereas the dependence $z_{\text{out}}-z_{\text{in}}$ is a regular one in the vicinity of $z_{\text{in}} \simeq 0$. With increasing the detection time (see Fig. 5b at $\tau = 200$), the probability of detecting any value of z_{out} in the interval $[-1, 1]$ is almost unity in the whole range of z_{in} . The formula (32) gives the value of the predictability horizon $\tau_p \simeq 200$ with $\lambda \simeq 0.05$. To feel the difference, it is desirable to carry out a control experiment at the exact resonance ($\delta = 0$) when the atomic motion is fully

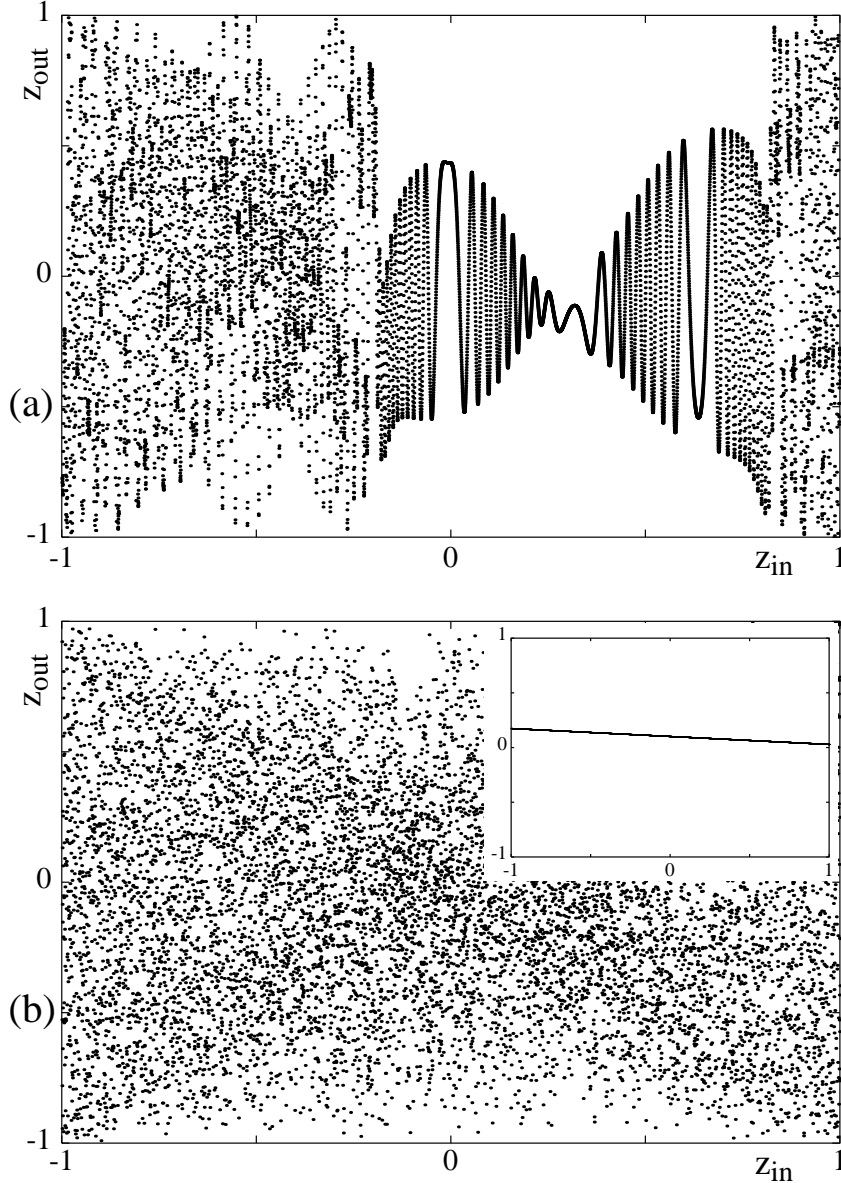


Fig. 5. Dependence of the output values of the atomic population inversion z_{out} on its initial values z_{in} with $\delta = 0.4$ (a) at $\tau = 100$ and (b) at $\tau = 200$ with the inset showing this dependence at the exact atom-field resonance, $\delta = 0$.

regular with any initial values. The dependence $z_{\text{out}}-z_{\text{in}}$ with $\delta = 0$ is demonstrated in the inset in Fig. 5b with all the other control parameters and initial values being the same.

4.4 Atomic fractals in a quantized field

In this section, we treat the atom-photon interaction in a high-Q cavity as a chaotic scattering problem [19,20]. Atoms from outside are injected into a

1D-cavity, interact for a while with the cavity field and then they are removed from the cavity by hook or by crook. Following to [5,11], let us consider the scheme of scattering of atoms by the standing wave shown in Fig. 4b. Atoms, one by one, are placed at the point $x = 0$ with different initial values of the momentum p_0 along the cavity axis. For simplicity, we suppose that they have no momentum in the other directions (1D-geometry). We compute the time the atoms need to reach one of the detectors placed at the cavity mirrors. The dependence of this exit time T on the initial atomic momentum p_0 is studied under the other initial conditions and parameters being the same. To avoid complications that are not essential to the main theme of this section, we consider the cavity with only two standing-wave lengths. Before injecting into a cavity, atoms are suppose to be prepared in the superposition state with $u_{n-1}(0) = u_n(0) = v_{n-1}(0) = v_n(0) = 0$, $z_{n-1}(0) = -1/2, z_n(0) = 1/2$, i. e. in the state with zero population inversion $z(0) = z_{n-1}(0) + z_n(0) = 0$.

At exact resonance ($\delta = 0$) with $u_{n-1}(\tau) = u_n(\tau) = 0$, the optical potential $U = (\sqrt{\bar{n}} u_{n-1} + \sqrt{\bar{n} + 1} u_n) \cos x - \delta(z_{n-1} + z_n)/2$ is equal to zero, and the analytical expression for the dependence in question can be easily found to be the following: $T(\delta = 0) = 3\pi/2\alpha p_0$ if $p_0 > 0$ and $T(\delta = 0) = \pi/2\alpha p_0$ if $p_0 < 0$. Atoms simply fly through the cavity in one direction with their initial constant velocity and are registered by one of the detectors. Out of resonance ($\delta \neq 0$), the atomic motion has been numerically found in the preceding section to be chaotic with positive values of the maximal Lyapunov exponent. Fig. 6 shows the function $T(p_0)$ with the normalized detuning $\delta = 0.4$, the recoil frequency $\alpha = 10^{-3}$, and the average initial number of cavity photons $\bar{n} = 10$. The exit-time function demonstrates an intermittency of smooth curves and complicated structures that cannot be resolved in principle, no matter how large the magnification factor. Fig. 6b shows magnification of the function for the small interval $64.1 \leq p_0 \leq 64.6$. Further magnification in the range $64.2743 \leq p_0 \leq 64.2754$ shown in Fig. 6c reveals a beautiful self-similar structure. Some structures in Fig. 6a that look like fractal are not, in fact, unresolvable and self-similar. Magnification of the structure in the range $73.2 \leq p_0 \leq 73.8$ (Fig. 7a), shown in Fig. 7b, demonstrates quite a smooth function without unresolvable substructures and with only two singular points on the borders of the respective momentum interval. Beating, visible in all the structures of the atomic fractal in Figs. 6, 7, should be attributed to the structure of the Hamilton-Schrödinger equations (24) which describe two atom-field oscillators with slightly different frequencies.

The exit time T , corresponding to both smooth and unresolved p_0 intervals, increases with increasing the magnification factor. It follows that there exist atoms never reaching the detectors in spite of the fact that they have no obvious energy restrictions to leave the cavity. Tiny interplay between chaotic external and internal dynamics prevents these atoms from leaving the cavity. The similar phenomenon in Hamiltonian systems is known as *dynamical trap*-

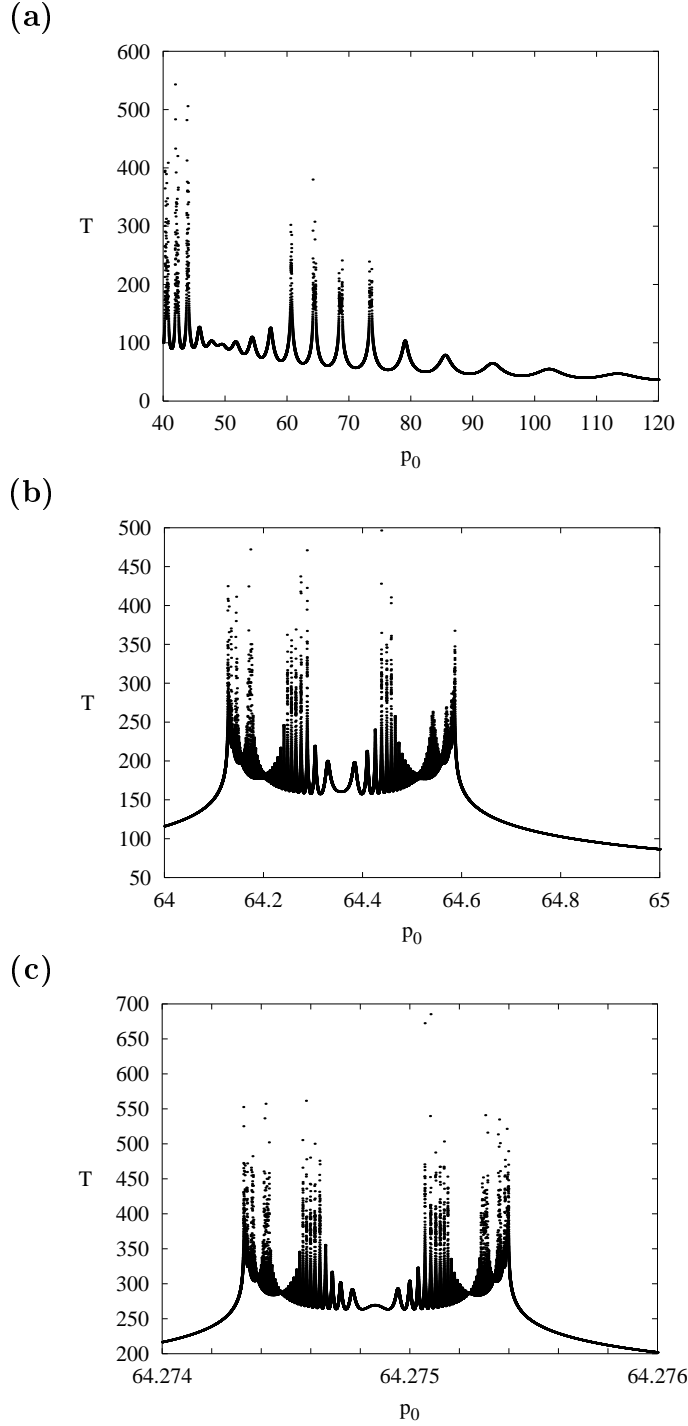


Fig. 6. Atomic fractal in a quantized Fock field with different resolutions ($\delta = 0.4$ and $z(0) = 0$).

ping [16]. Different kinds of atomic trajectories, which are computed with the system (24), are shown in Fig. 8. A trajectory with the number m transverses the central node of the standing-wave, before being detected, m times and is called m -th trajectory. There are also special separatrix-like mS -trajectories following which atoms in infinite time reach the stationary points $x_s = \pm\pi n$

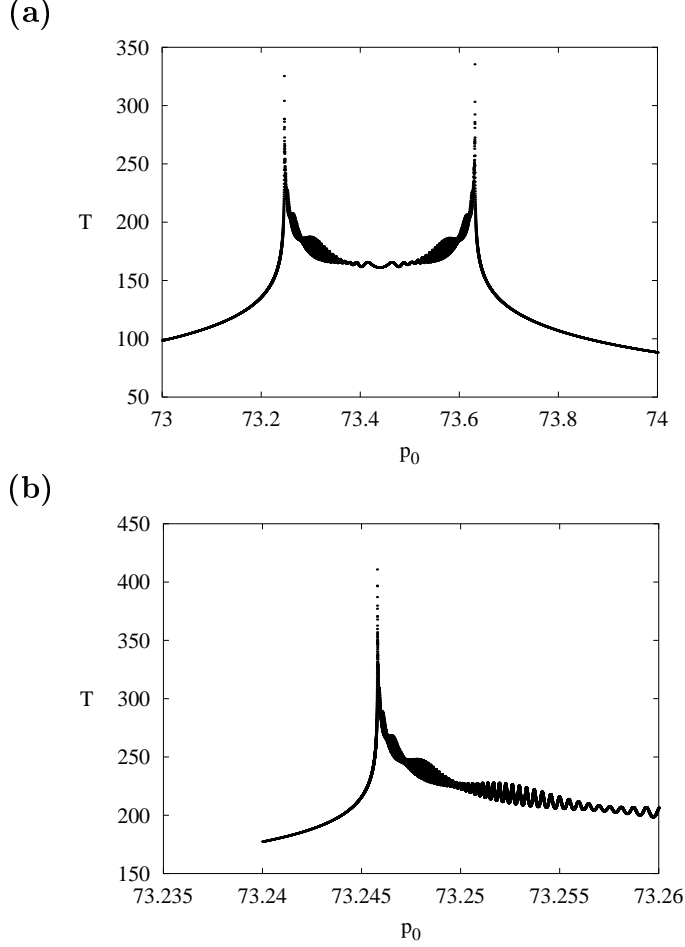


Fig. 7. Example of one of the non-fractal substructures in the atomic fractal shown in Fig. 6a with successive magnifications.

($n = 0, 1, 2, \dots$), $p_s = 0$, transversing m times the central node. These points are the anti-nodes of the standing wave where the force acting on atoms is zero. A detuned atom can asymptotically reach one of the stationary points after transversing the central node m times. The trajectory with number 1, showing in Fig. 8, is close to a separatrix-like $1S$ -trajectory. The smooth p_0 intervals in the first-order structure in Fig. 6a correspond to atoms transversing once the central node and reaching the right detector. The unresolved singular points in the first-order structure with $T = \infty$ at the border between the smooth and unresolved p_0 intervals are generated by the $1S$ -trajectories. Analogously, the smooth and unresolved p_0 intervals in the second-order structure in Fig. 6b correspond to the 2-nd order and the other trajectories, respectively, with singular points between them corresponding to the $2S$ -trajectories and so on.

There are two different mechanisms of generation of infinite exit times, namely, dynamical trapping with infinite oscillations ($m = \infty$) in a cavity and the separatrix-like motion ($m \neq \infty$). The set of all initial momenta generating

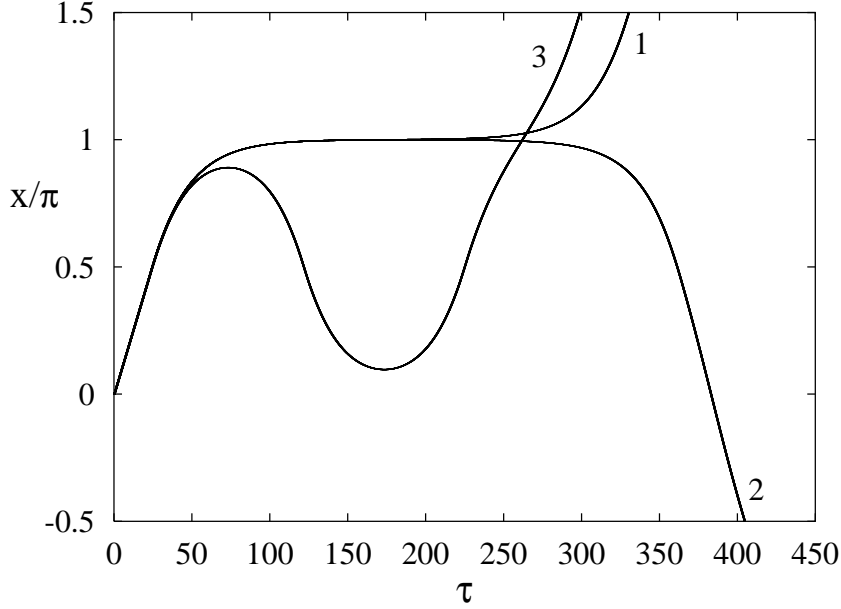


Fig. 8. Sample atomic trajectories transversing the central node in the scheme Fig. 4b m times ($m = 1, 2, 3$). The trajectory with number 1 is close to a separatrix-like $1S$ -trajectory.

the separatrix-like trajectories is a countable fractal. Each point in the set can be specified as a vector in a Hilbert space with m integer nonzero components. One is able to prescribe to any unresolved interval of m -th order structure a set with m integers, where the first integer is a number of a second-order structure to which trajectory under consideration belongs in the first-order structure, the second integer is a number of a third-order structure in the second-order structure mentioned above, and so on. Such a number set is analogous to a directory tree address: “<a subdirectory of the root directory>/<a subdirectory of the 2-nd level>/<a subdirectory of the 3-rd level>/...”.

5 Conclusion

Atoms in cavities provide a microscopic nonlinear dynamical system with a reach variety of qualitatively different dynamics that may be explored to study the key problems of modern quantum physics and nonlinear science including the problem of the quantum-classical correspondence. The up-to-date experimental state of art has reached the stage where the quantum to classical transition and the borderland between them can now be probed directly. Increasing the number of atoms or/and the average number of photons in a cavity mode, one can force the atom-field system to operating in quantum, semiquantum, and semiclassical regimes providing a link between micro-, meso-, and . In this paper, we derived the Hamilton – Schrödinger equations of motion that

describe the semiquantum Hamiltonian dynamics of a two-level atom with recoil strongly coupled to a single-mode standing-wave quantized field in an ideal cavity. It has been shown that dynamical chaos and fractals may arise in a wide range of the control parameters of the system. To estimate their magnitudes we use the parameters of the real experiments with single atoms in Fabry – Perot microcavities in the strong-coupling regime [18], for which the amplitude of the atom-field coupling strength may reach $\Omega_0 = 2\pi \cdot (10^7 \div 10^8)$ Hz exceeding the decay rates of the cavity mode and the atomic dipole. With the above mentioned values of Ω_0 and $k_f \simeq 2\pi \cdot 10^6 \text{ m}^{-1}$, one can estimate the normalized recoil frequency α to be in range 10^{-5} – 10^{-2} depending on the magnitude of the atomic mass.

Acknowledgments

This work was supported by the Russian Foundation for Basic Research under Grant Nos. 02–02–17796, 02–02–06840, and 02–02–06841. One of the authors (S. P.) thanks the Organizing Committee of the Workshop for supporting his visit to Carry le Rouet.

References

- [1] B.V. Chirikov, Phys. Rep. **52**, 263 (1979); G.M. Zaslavsky, Phys. Rep. **80**, 157 (1981).
- [2] E.T. Jaynes, F.W. Cummings, Proc. IEEE **51**, 89 (1963).
- [3] S.V. Prants, L.E. Kon'kov, Phys. Lett. A **225**, 33 (1997).
- [4] S.V. Prants, L.E. Kon'kov, and I.L. Kirilyuk, Phys. Rev. E **60**, 335 (1999).
- [5] S.V. Prants, Pis'ma Zh. Éksp. Teor. Fiz. **75**, 777 (2002) [JETP Letters **75**, 651 (2002)].
- [6] L.E. Kon'kov, S.V. Prants (unpublished).
- [7] V.G. Minogin, V.S. Letokhov, *Laser Light Pressure on Atoms*, Gordon and Breach, New York (1987); A.P. Kazantsev, G.I. Surdutovich, V.P. Yakovlev, *Mechanical Action of Light on Atoms*, World Scientific, Singapore (1990).
- [8] S.V. Prants, L.E. Kon'kov, Pis'ma Zh. Éksp. Teor. Fiz. **73**, 200 (2001) [JETP Lett. **73**, 180 (2001)].
- [9] S.V. Prants, V.Yu. Sirotkin, Phys. Rev. A **64**, 033412 (2001).
- [10] S.V. Prants, Pis'ma Zh. Éksp. Teor. Fiz. **75**, 71 (2002) [JETP Lett. **75**, 63 (2002)].

- [11] S.V. Prants, V.Yu. Argonov, e-print archive, physics/0206005.
- [12] S.V. Prants, M. Edelman, and G.M. Zaslavsky, Phys. Rev. E (in press).
- [13] V.Yu. Argonov, S.V. Prants, Zh. Éksp. Teor. Fiz. (in press).
- [14] G.M. Zaslavsky, R.Z. Sagdeev, D.A. Usikov, and A.A. Chernikov, *Weak Chaos and Quasiregular Patterns* (Cambridge University Press, Cambridge, England, 1991).
- [15] G.M. Zaslavsky, *Physics of Chaos in Hamiltonian Systems*, Imperial College Press, London (1998).
- [16] G.M. Zaslavsky, Physica D **168-169**, 292 (2002).
- [17] V.I. Ioussoupov, L.E. Kon'kov, and S.V. Prants, Physica D **155**, 311 (2001).
- [18] C.J. Hood, T.W. Lynn, A.C. Doherty, et al, Science **287**, 1447 (2000); P. Münstermann, T. Fischer, P. Maunz et al, Phys. Rev. Lett. **82**, 3791 (1999).
- [19] E. Ott, *Chaos in Dynamical Systems*, Cambridge University Press, Cambridge (1993).
- [20] R. Blümel, W.P. Reinhardt, *Chaos in Atomic Physics*, Cambridge University Press, Cambridge (1997).